Differential RNA-silencing and plasmodesmata callose deposition in leaves and stems of transgenic tobacco plants during *Tobacco etch virus* infection recovery

Pablo Vargas-Mejía[a], Alejandro Olguín-Lamas[a], Selene L. Fernandez-Valverde[b], Gertrud Lund[a], Jean-Philippe Vielle-Calzada[b], and Laura Silva-Rosales[a]#

[a]Departamento de Ingeniería Genética, Centro de Investigaciones y de Estudios Avanzados, Unidad Irapuato, Guanajuato, Mexico.

[b]Unidad de Genómica Avanzada, Cinvestav, Irapuato, Guanajuato, Mexico.

Running Head: RNA-silencing in tobacco during TEV recovery

#Address correspondence to Laura Silva laura.silvar@cinvestav.mx

Abstract word count: 216

Importance word count: 94

Text word count: 4667

ABSTRACT

Viruses are amongst the most prevalent pathogens that threaten plants. Plants have evolved a sequence-specific defence mechanism against viruses to ensure survival, known as RNA silencing, which includes transcriptional and post-transcriptional gene silencing. After a viral infection, plants can undergo the process of recovery, and become further resistant to viral infection after a new systemic infection. This study aimed to identify additional mechanisms underlying disease recovery besides the known RNA silencing. Thus, we analyzed the transgenic tobacco plants for the *tobacco etch virus* (TEV) expressing a transcript derived from the Nuclear Inclusion "a" protein (NIa) cistron of TEV, which had recovered from infection three weeks following viral inoculation. Performing *in situ* hybridizations, we detected the virus and the transgene-derived transcript in stem sections adjacent to the recovered leaves. To further understand the silenced and non-silenced conditions in leaf and stem, we undertook tissue-specific RNA-Seq and small RNA-Seq analyses in these tissues, and found a higher number of differentially expressed genes (DEGs) in the recovered leaf related to defence, silencing, and hormone signaling responses. Finally, we observed differences in plasmodesmata callose deposition and callose-related genes. Overall, the findings of the present study suggest that cell-to-cell viral restriction movement also participates in the recovery of TEV infection in transgenic tobacco plants, besides the key function of RNA silencing.

IMPORTANCE

Host recovery from a viral infection is a common strategy to ensure survival. In plants and other eukaryotes, this phenomenon has been strongly related to RNA silencing. However, the role of other defense mechanisms remains unexplored. Recovery has been studied in

leaves where is visually observed. The implications of other organs such as the stem remain poorly understood. We give insights into differential RNA silencing occurring between leaves and stems. This study demonstrated that additional mechanisms, such as overexpression of defense-related genes and callose accumulation in plasmodesmata, during recovery are involved, besides RNA silencing.

KEYWORDS: potyvirus; Tobacco etch virus (TEV); RNA silencing; plant-virus interaction; recovery; RNAseq; callose deposition

INTRODUCTION

Plants have developed specialized strategies to ensure survival in response to constant biotic and abiotic threats. Such strategies include innate and adaptive immune responses involving components of the systemic acquired resistance (SAR) and the RNA interference (RNAi) machinery, respectively (1, 2). Viruses, together with fungi and bacteria, are among the most prevalent pathogens. One of the outcomes of viral infection in plants is symptom recovery, characterized by the emergence of asymptomatic leaves at the apex after systemic symptomatic infection occurrence. Such leaves are virus-free and remain resistant to new inoculation of the same or highly related viruses. Recovery from viral disease was first documented in 1928 (3); later, in 1993, was linked to the RNA silencing machinery (4–6), and recently, RNA silencing indeed was proposed as the primary mechanism of viral recovering leaves (5). Recovery occurs naturally in wild-type plants, especially those infected with positive-sense single-stranded (ss+) RNA viruses and DNA viruses like geminivirus, as well as in those transgenic plants expressing coding or non-coding sequences of the virus genome (7–9).

RNA silencing is a conserved sequence-specific defence mechanism against viruses that includes transcriptional (TGS) or post-transcriptional gene silencing (PTGS) (10, 11). PTGS results in the production of small RNAs with the participation of RNA-dependent RNA polymerases (RDRs) producing dsRNA, which are recognized and cleaved by Dicer-like 2,4 (DCL2,4) (12, 13). The dsRNAs can also result from secondary RNA structures formed during viral genome replication. Cleaved 21-24nt products are small interfering RNAs (siRNA) that associate with argonaute AGO1 and AGO2 proteins and bind to the RNA-induced silencing complex (RISC) to identify and cleave targets with complementarity sequence to the AGO-associated siRNA (14). RDRs can also participate in amplifying the RNA-silencing signal through the vascular system by synthesizing new dsRNA from aberrant RISC-cleaved RNAs recruited by SGS3. Viruses have evolved proteins that counteract silencing by siRNAs, known as VSRs (Viral Silencing Repressors), by sequestering virus-derived small RNAs and inhibiting their incorporation into the RISC complex. They can also interfere with the expression of the plant silencing machinery through the inactivation or destabilization of RNAi and proteins or by promoting the expression of host endogenous suppressors or regulators of RNA silencing (ESRs). Nbrgs-CaM (calmodulin from *Nicotiana benthamiana* repressor of gene silencing) is the first example of an ESR. The RNAs of viruses encoding weak VSRs, or transgenic plants producing low levels of transgene-derived transcripts, are complemented with the virus-derived transcripts to surpass the RNA threshold level necessary to trigger recovery (6, 8, 15).

Recovery of viral infection mediated by RNA silencing has been studied in leaves as this is the site where recovery is visually observed. Some authors suggested the existence of an elusive systemic RNA-silencing signal (16). The existence of such signal involves a poorly

understood organ: the stem. We are not aware of research involving the participation of this organ, a key component in systemic viral movement, and the search for its participation during recovery is addressed to understand the systemic nature of the process of recovery in plants. Here, we searched for RNA silencing participants in the stem and leaf during the final stage of recovery and for other genes that might be differentially expressed in the two organs to help to understand plant systemic recovery in transgenic plants after viral infection. Therefore, this study aimed to identify additional mechanisms underlying disease recovery besides the known RNA silencing observed in the leaves.

RESULTS

NIa-transgene expression and recovery

Following TEV infection, transgenic NIa tobacco plants developed a systemic infection characterized by typical mosaic symptoms in the inoculated leaf and also in the three leaves immediately above the inoculated leaf. The process of recovery (PR) was first observed in the interveinal regions of the leaf above the inoculated one (Nla-PR1). Between 14 to 21 days post-inoculation (dpi), the PR progressively increased in leaves 2 (NIa-PR2) and 3 (NIa-PR3), *i.e.*, NIa-PR1< NIa-PR2< NIa-PR3, registering a complete recovery in leaf 4 (NIa-R4) (Fig. 1a). Once recovered, the leaves remained highly resistant to the virus. In contrast, all the leaves of WT plants remained symptomatic, while those of mock-inoculated NIa tobacco (NIa-N1-4) presented a normal development (Fig. 1b, c, respectively). As expected, no infection was observed when recovered leaves were used as a source of inoculum in healthy plants (Figure S2).

PTGS was involved in transgenic NIa-tobacco recovery

We confirmed that the PR observed in leaves of NIa plants resulted from PTGS. By Northern blot, the expected 1290 nt band corresponding to the NIa RNA transcript was increased ~20 fold in NIa-N1-3 compared to NIa-PR1-3 leaves (Fig. 1d). Also, nuclear transcription rates of the transgene-derived NIa cistron and the endogenous ubiquitin gene were similar in unchallenged and recovered tissue at a similar physiological stage (NIa-N3 and NIa-PR3 at 21 dpi, integrated density values, IDV = 1.99 and 2.20, respectively). The multiple bands in the ubiquitin control lane resulted from incomplete digestion of the plasmid blotted onto the membrane (Fig. 1e). This indicated that NIa transgene expression is similar in both the nuclei of plants in process of recovery and mock plants and that recovery and viral gene silencing were activated following virus replication in the cytoplasm (Fig. 1e). The presence of the viral transgene-derived transcript in the nucleus and its absence in the cytoplasm indicated that PTGS was acting in the recovery process.

Stem and leaf-vascular tissue did not undergo silencing as shown by *in situ* hybridization

We used the antisense viral NIa segment as an RNA probe to detect viral and/or transgene-derived transcripts in the leaf blade and leaf stem base, *i.e.*, the area of the stem that connects to the petiole, of NIa-N and NIa-PR plants by *in situ* hybridization (Fig. 2). A positive signal in NIa-N tissues indicated the presence of the transgene-derived transcript, while the corresponding signal in NIa-PR tissues indicated the presence of viral transcript due to infection. In the leaf blade, we observed transgene-derived transcript in NIa-N1-3 leaves (Fig. 2a). Whereas very faint or no signal was detected in NIa-PR leaves (Fig. 2a, c, respectively), indicative of RNA silencing for both the viral-derived transcript and the virus. No signal was observed in the corresponding NIa-PR1-3 leaves. Conversely, viral and/or transgene

expression at the stem was observed in both mock and viral inoculated NIa plants (Fig. 2b, d). In mock plants, we observed a strong transcript signal in all cell types, including upper and lower epidermis, palisade, and spongy parenchyma, with higher intensity in the nucleus. Vascular bundles also presented a strong transcript signal. In the stem, phloem cells (companion cells and sieve elements), showed evidence of the transgene-derived transcript (Fig. 2a, b). In some areas, phloem parenchyma cells were also indicative of the presence of the transcript.

Stem and leaves cut sections of NIa-PR3 were used as the source of inoculum in healthy plants, those infected with NIa-PR3 leaves remained uninfected. Meanwhile, plants infected with NIa-PR3 stems developed a symptomatic TEV infection, validating the *in situ* hybridization observation of TEV-free leaves and infected stems (Figure S2).

As expected, mock-inoculated WT B49 plants showed no evidence of viral expression in the leaf or stem. In contrast, the inoculated counterparts showed hybridization profiles similar to mock-inoculated NIa plants, albeit with a slight reduction of virus signal in leaves 2 and 3 (Figure S3).

The boundary zone at the stem-petiole insertion presented a differential accumulation of viral transcript in the RNA NIa signal (Fig. 3). For instance, NIa RNA accumulated in the stem rather than in the petiole, except for the petiole vasculature, where NIa RNA was present (Fig. 3a). Likewise, NIa was present in the leaf vasculature but not in the mesophyll tissue when we analyzed longitudinal sections of the leaf (Fig. 3b).

Methylation analysis revealed no implication of the TGS mechanism in the process of recovery

Bisulfite-treated DNA was obtained from leaves and stems of mock- (NIa-N4 and N1a-N3) or TEV- (NIa-R and NIa-PR3) inoculated plants, and the PCR amplification products

obtained using either of the specific primers designed are shown in Figure S4. Considering the ratio between PCR products of unmethylated and methylated primer pairs, we found that the promoter sequence was more methylated than non-methylated in both and leaf tissue; yet, presented higher levels in the latter and in particular in NIa-N3 NIa-PR3 leaves (Figure S5). Indeed, bisulfite sequencing analysis of 8-10 individual cloned PCR products from N1a-N4, NIa-R and NIa-PR3 leaves, showed that the latter was characterized by an increase in CG, CHG and CHH methylation (Figure S5). Contrary to the expected, methylation was higher in the leaf than in the stem for the promoter of PR3 and R stage, indicating that viral silencing was not compromised by transgene down-regulation in the stem.

Defence-related genes were overexpressed in leaf

To explore leaf and stem-specific responses to TEV during recovery, we performed high throughput RNA sequencing using transgenic NIa-plants at the PR3 stage. We identified 731 differentially expressed genes (DEGs) (log2FC $\geq$1 and $\leq$-1 and q-value of $\leq$0.05); among them, 700 DEGs corresponded to the leaf and 31 DEGs to the stem. Functional enrichment analysis of the identified DEGs resulted in enrichment for the “binding” molecular function (MF) in the stem. On the other hand, 16 enriched biological processes (BP) were identified in the leaf, including “defence response”, “regulation of RNA metabolism”, “protein phosphorylation”, and “ubiquitination” (Fig. 4). Similarly, 17 MFs including “oxidoreductase activity”, “protein binding”, “sequence-specific DNA binding”, and “transcription factor activity” were enriched in this tissue. Overall, we found 28 disease resistance, 8 jasmonic acid, and 3 ethylene-related genes differentially expressed in the leaf (Table S1), whereas no defence-related genes were differentially expressed in the stem.

Silencing machinery was overexpressed in the leaf while suppressors of silencing were overexpressed in the stem

As silencing has been reported as the principal mechanism of recovery, we analyzed nine key silencing genes (DCL2, DCL4, SGS3, HEN1, NRPD1a, RDR6, RDR2, AGO1, and AGO2) searching for differential expression. We found that four of the nine key silencing genes, namely AGO1, DCL2, HEN1, and RDR6, were overexpressed in the leaf compared to the stem (Table 1). The other five genes were not differentially expressed. Moreover, in the stem, we found one transcript encoding for the calmodulin-binding protein-like (rgs-CML), which is a virus-triggered endogenous suppressor of RNA silencing well-characterized in tobacco (Table 1).

Callose accumulation in the leaf suggested restriction of viral cell-to-cell movement by plasmodesmata

We further analyzed differences in the presence of transcripts in tissues that are involved in the viral movement. In this vein, we found that genes encoding for enzymes related to callose synthesis (three glucan synthase-like enzymes —GSL, and one callose synthase —CALS), and callose accumulation (five callose accumulation at plasmodesmata) were overexpressed in the leaf (Table 2). In line with these results, we also found a major accumulation of callose at leaf plasmodesmata compared to the stem of NIa-plants at the PR3 stage (Fig. 5).

Plant miRNA and vsiRNA profiles

A total of 12 miRNA were detected to be differentially expressed (p-value ≤ 0.05) in the leaf and 4 in the stem, with 77 and 6 predicted targets, respectively. Functional enrichment analysis of leaf miRNAs targets showed a negative regulation of macromolecule

modification and protein phosphorylation (Fig. 6a) with miRNA targets of plant-pathogen interaction pathway and disease resistance (Table S2). Meanwhile, enrichment for stem miRNA did not show any enriched GO term.

Whereas virus-derived small interfering RNAs (vsiRNAs) are commonly produced during viral infections, and work as keystone molecules for effective viral silencing. In this study, we observed vsiRNA mostly accumulated in the stem rather than in the leaves (489.89 CPMx10^{-3} and 448.96 CPMx10^{-3}, respectively). However, the 24nt vsiRNAs were more abundant in the leaf, even when DCL3 was not differentially expressed in this tissue (Fig. 6b, Table 1). TEV genome-wide accumulation of vsiRNAs revealed *per-site* differences, with more abundance at the P1 cistron than other genomic regions, including the NIa transgene (Fig. 6c). Log2 Fold change was calculated to compare vsiRNA genome accumulation between leaf and stem. We found a lower vsiRNA accumulation in the leaf (Figure S7). In addition, we found remarkable differences in the negative-stranded vsiRNA of P3 and CI cistrons between leaf and stem, suggesting these RNAs could be important in maintaining a non-silenced stem (Figure S7b).

It has been proposed that vsiRNA has the potential to regulate host gene expression (17) Therefore we investigated if vsiRNA derived from abundant sites and P3, CI cistrons have host gene targets. As a control, we evaluated 30 random non-abundant vsiRNA sites. Although we found tobacco targets for both abundant and non-abundant vsiRNA sites, after functional enrichment analysis we didn't find enrichment for abundant or non-abundant regions. However, for the P3 cistron region between ~3200-3300nt (-), we found stem-derived-vsiRNA target GSL03 gene involved in viral movement restriction. On the other hand, vsiRNA present as peaks at the P1 and HC-Pro (~900nt and ~1600nt) region had DCL4

and PR1 amongst their targets. No defence-related target genes were found in the non-abundant regions.

DISCUSSION

Plants undergo a process of recovery which is compartmentalized

Stems cuttings from recovered plants of vegetative crops can propagate virus-free plants. This phenomenon was described as reversion, and it was concluded that virus distribution is restricted in recovered plants (18, 19). Even when reversion and recovery terms have been used as the same, recovery stands for a plant previously infected showing symptoms, while reversion refers to a symptom-free recovered plant. We observed that the process of recovery in leaves of NIa plants resulted from PTGS, as in other recovery and reversion systems (5). And that recovered tissues remain highly resistant to the virus as reported before with other transgenic tobacco plants expressing the TEV-viral coat protein cistron (20). The presence of the virus in the stem and leaf vasculature but not in the mesophilic cells suggested restriction of intracellular movement of TEV, possibly occurring in the exit from the phloem (Fig. 3).

Some works showed that not all the new emerging organs are fully recovered, similar to what we saw between the recovered leaves and non-recovered stem in the present study, these indicates that the processes of recovery and reversion imply different molecular mechanisms. However, none of these works compared the differences between recovered and non-recovered tissues (21, 22).

RNA silencing and viral movement restriction at leaf and stem

It's well known that RNA silencing plays a key role in recovery as the elimination of components of the RNA silencing machinery halts plant recovery (21, 23). Viruses that efficiently counteract RNA silencing evade recovery (24, 25). Here we found that genes that are essential for RNA silencing, including AGO1, DCL2, HEN1, and RDR6, were overexpressed in the leaf but not in the stem. Interestingly, AGO2 was not differentially expressed, albeit described as the main silencing gene involved in antiviral defence (14). Other key genes for VIGS and siRNA biogenesis, such as SGS3 and SDE5, were not differentially expressed; even those key genes related to PTGS-TGS crosstalk, such as NRPD and RDR2, were neither differentially expressed (23, 26, 27). These findings suggest that other factors may be involved in the stem repression of silencing since some key silencing-related genes are equally expressed in both tissues (DCL4, SGS3, NRPD1a, RDR2, and AGO2). In this vein, we found the plant endogenous rgsCaM was overexpressed in the stem, suggesting it may participate in silencing suppression in this tissue since it is known to be recruited by TEV HC-Pro to suppress RNA silencing (28); this outcome may also explain the lower expression of RDR6 (29). Moreover, rgsCaM has also been attributed to enhancing the resistance by targeting itself and the HC-Pro to proteolytic pathways, as so restricting viral infections to local areas. In this sense, the overexpression of rgsCaM could explain the lack of silencing in the stem and enhancement of antiviral responses restricting viral infection to this tissue (30). Still, the question of whether these responses would happen in a non-transgenic system persists.

Plant innate immunity also participates in plant recovery

Exclusion from tissues such as meristem has been attributed to RNA silencing and is considered a key step in viral recovery (31). Recent works provide evidence that silencing is

not the reason for tissue exclusion of this response as DCL2/4-silenced plants infected with CymRSV were free of the virus at the meristem (32). Most of the literature describes recovery by specific components in the RNA silencing pathway rather than considering the global changes occurring in a plant during the recovery process. However, PAMP-triggered immunity (PTI) has been reported to be prevalent in almost all plant-virus transcriptomes. In this vein, we detected many genes involved in PTI and canonical defence were overexpressed in the leaf. For instance, nine genes related to callose deposition at plasmodesmata or negative regulators of plasmodesmata permeability (GSL12, GSL1, GSL03, CALS1, CAD1, IRX1, PEN3, UGT74B1, and CESA4) were overexpressed in the leaf. Further corroboration of callose accumulation by image microscopy, let us confirm this presumption. Similar to our findings, a Cassava resistant line to CBSV allowed viral transmission through the stem whereas no virus could be detected in leaves (33). Also, in the following study, the authors found overexpression of b-1,3-GLUCANASE, ANKs, and PDLP1 genes in the susceptible line. These genes participated in plasmodesmata permeability or as the viral movement-promoting factors, whereas GSL4 (a possible negative regulator of plasmodesmata permeability) was overexpressed in both susceptible and resistant lines (34). However, we did not find any viral movement promotor overexpressed in the stem, which may suggest that in our system a different viral movement restriction system takes place compared to CBSV-resistant Cassava one.

vsiRNA accumulation at leaf and stem

Contrary to the findings in ORMV-infected Arabidopsis plants that showed a high amount of 21-22nt vsiRNA accumulated in recovered leaves that presented active-infectious virus (23), in the present study we observed that the recovered tissue (leaf) presented a lower

amount of 21-23nt vsiRNA compared to the non-recovered stem. Out of the 7 genes dubbed crucial for recovery (23, 27) we found 4 (AGO1, DCL2, HEN1, and RDR6 overexpressed in the leaf as compared with the stem. The higher accumulation of vsiRNAs at the stem could be explained by the active replication of the virus in this tissue. Despite the overexpression of DCL2 (involved in 22nt production) in leaves, we found more accumulation of 24nt than 21-23nt vsiRNAs. Because it is more common that 21-22nt vsiRNAs accumulate in higher amounts than 23-24nt vsiRNAs during viral infections (35, 36), further investigation needs to be performed to explain our differential findings. Moreover, the higher accumulation of positive vsiRNAs seems to be common in positive-stranded RNA viruses, a condition also noticed in this study (35). The non-random distribution of vsiRNAs along the TEV genome is also common and is associated with the fold-back structures of the genomic RNA and binding of the vsiRNAs to the viral HC-Pro (37–39). Those accumulation hotspots were associated with pathogenesis modulation by vsiRNA in the host machinery (17). However, we did not find vsiRNAs host targets involved in defense response or the pathogenesis-related when we looked for targets within the 20 highest hotspots, even when we look for the high fold-change accumulation hotspots between leaves and stem.

CONCLUSIONS

This study demonstrated that additional mechanisms, such as overexpression of defence-related genes and callose accumulation in plasmodesmata, underly the viral disease recovery besides RNA silencing. Even more, we bring insights that compartmentalization or specialization differentially occurs between leaves and stems since RNA silencing and plant defence responses are mounted to a different extent in such tissues. Thus, this study opens the window to start investigating whether defence responses (innate and adaptive) to viruses

or even other pathogens are also differentially triggered in other plant organs. Understanding this compartmentalization would allow the designing of new strategies to control diseases.

MATERIALS AND METHODS

Plant transformation

The viral NIa cistron sequence was initially cloned into the BamHI sites of plasmids pTL37/8595 containing both T7 and SP6 promoters (20). Haploid leaf tissue from plants of *Nicotiana tabacum* cultivars B49 and K326 were transformed via *Agrobacterium tumefaciens* (40). Convenient restriction sites were also engineered (*e.g.*, NcoI, BamHI, and PstI). A wide host range plasmid pPEV6 containing T-DNA borders, NIa gene, and the neomycin phosphotransferase II gene (that confers kanamycin resistance) selectable marker were mobilized from *E. coli* into *A. tumefaciens* as described previously by Smith et al. (1994) and used to transform tobacco tissue. Transformed tissue was selected in the presence of 100 µg/mL of kanamycin sulfate, and doubled haploid plants were obtained from haploid mid-vein cultures (41). These plants were allowed to seed, and seeds were used for further studies. Burley 49 transformed plants are referred to as NIa.

Transgene expression

Transgenic seed screening was performed as described before (9). To detect the transcript containing TEV NIa sequences, total leaf RNA was isolated using phenol:chloroform. Denaturing formaldehyde gels were blotted onto nylon membranes and hybridized with antisense 32P-labeled RNA probes. Such probes were obtained by an *in vitro* cell-free transcription system of plasmid pTL37/8595, containing the NIa gene insert, using SP6 RNA polymerase.

Nuclear run-off assays

Isolation of nuclei from non-transformed and transgenic plant tissue was performed according to (42) with a slight modification in the amount of starting tissue (we used 3 g of leaves). DNA plasmids containing either the NIa insert, or the resident gene ubiquitin were digested using HindIII restriction enzyme. Then, 5 µg of the restricted products were electrophoresed in an agarose gel and then blotted onto nylon membranes. Labelled 32P-RNA transcripts for run-off reactions were added in equal amounts (estimated by specific counts per million CPM) and used to hybridize the membranes containing DNA plasmids.

Inoculation of transgenic plants

In three independent replicates, 10 plants from each line were inoculated when reached approximately 30 cm tall. Plant leaves were lightly dusted with carborundum and a 1:3 dilution of virus inoculum was applied with a cotton swab (dilution in w/v of virus-infected plant tissue in deionized distilled sterile water). Plant viral symptoms were daily recorded after the positive control plants started to show symptoms (8-10 days after inoculation).

***In situ* hybridization**

In situ hybridization was performed as described (43) with modifications. For the synthesis of sense and anti-sense 11-digoxigenin-UTP labelled probes, a pTC plasmid containing a 1290-bp NIa fragment was linearized with restriction enzymes PsT I, and 1 µg was used as a template for probe synthesis. RNA probes were synthesized using DIG northern starter kit (Roche, Mannheim, Germany). Transgenic non-inoculated (NIa-N plants) or TEV-inoculated and in process of recovery (NIa-PR1-PR3 and R) were fixed as described by (44).

RNA probes were hydrolyzed following the method described by (43), and 3%–6% of each labelling reaction (100–400 ng of RNA) was mixed with 40 µl of 50% formamide, added to 200 µL of hybridization buffer, and used as a probe for a pair of slides. Overnight hybridization was performed as described by (44).

Total RNA extraction and Northern hybridization

For each 1.2 mg of total RNA, 50 µL of 5M NaCl and 63 µL of 40% PEG 8000 were added, and the final mixture was incubated on ice for 30 min. The supernatant was recovered after a 9000 rpm centrifugation at 4°C for 5 min, 500 µL of 25:24:1 phenol:chloroform:isoamyl alcohol was added, and followed by second centrifugation similar to the previous one. The aqueous phase was recovered after a standard 3M sodium acetate precipitation and the pellet was resuspended in DEPC-treated water. Total RNA was resolved on a denaturing 0.8% agarose gel. Gels were transferred to the HybondN+ membrane (Amersham, Piscataway, NJ, USA). Hybridizations were performed with viral-derived probes labelled with a dCTP32P.

Methylation analysis

To understand whether reduced viral expression in the leaf resulted from an increase in promoter methylation of the viral transgene, we designed primers pairs covering 103 bp of the cauliflower mosaic virus (CaMV) 35S promoter sequence, which drives the expression of NIa. Such primers were designed to amplify either unmethylated or methylated bisulfite-treated DNA and neither of those was capable of amplifying native DNA (data not shown). DNA extracted from NIa-N and PR leaves were treated with bisulfite (EZ DNA methylation gold, Zymo Research, Orange, CA, USA) before PCR amplification of the 35S promoter region of the CaMV. The primers' sequences were M_F:

AGGGTAATATCGGGAAATTTTTTCM and M_R: AAATCCATCTTTAAAACCACTATCG (for methylated DNA) and U_F: AAGGGTAATATTGGGAAATTTTTTT and U_R: ATCCATCTTTAAAACCACTATCAAC (for unmethylated DNA). Gel integrated density values (IDV) of PCR amplification products were obtained using the software ImageJ version 1.53c. Gene promoter DNA methylation profiling was carried out by sequencing 8 - 10 clones per DNA sample obtained by PCR amplification of bisulfite-treated genomic DNA and the percentage of CGN, CHG and CHH were analyzed using the tool CyMATE (45).

RNA extraction and Illumina Sequencing

Total RNA extraction was performed as described by (2). Briefly, tissue was collected from leaves or stems from 4 plants in process of recovery of PR3 and grounded in liquid nitrogen. A total of 4 RNA-Seq libraries (2 tissues, 2 replicates per tissue 2x100) were prepared and sequenced at Labsergen facilities (Irapuato, Mexico) using Illumina HiSeq2500 (Hayward, CA, USA). Raw data are publicly available at NCBI, BioProject accession: PRJNA844420.

Mapping and statistical analysis

Trimming and cleaning of reads were conducted according to (46). Mapping and quantification were made with Kallisto against the reference tobacco transcriptome Nitab-v4.5 (www.solgenomics.net) (47, 48). Kallisto was run with bias correction and 1000 bootstrap. Differential expression analysis was conducted with Sleuth (49). Reads of each library were mapped with a percentage of 81.05% pseudoaligned and 80.75% pseudoaligned just once to the transcriptome (Table S3). After the differential expression analysis,

transcripts with log2 FoldChange (log2FC) values of ≥1 and ≤-1 and q-value of ≤0.05 were considered as differentially expressed genes (DEGs).

Functional annotation and gene expression validation

To identify the Gene Ontology enrichment, Singular Enrichment Analysis (SEA) was performed with AgriGO v2 with the Nitab4.5 (www.solgenomics.net) background under Fisher and the multi-test adjustment method of Hochberg (FDR) with a p-value ≤0.05 (50). Ontology reduction and network construction were performed with REVIGO with standard parameters (medium 0.7 resulting list) and Cytoscape (51, 52).

Small RNA analysis

A total of 4 small RNA-Seq libraries (2 treatments, 2 replicates per treatment 1x36) were prepared with gel band selection and sequenced at Cinvestav facilities (CDMX, Mexico) using Illumina HiSeq2500 (Hayward, CA, USA). Raw data are publicly available at NCBI, BioProject accession: PRJNA844411. Reads were mapped with Bowtie 1.2.3 (--best --strata parameters) to the tobacco and TEV concatenated genomes, then miRNA prediction was carried out with ShortStack v3.8.5 standard parameters and we kept only those miRNA reported at miRBase (53). Differential expression analysis was carried out with DeSeq2 1.36.0 standard parameters and the target prediction of differentially expressed miRNA was carried out with psRNATarget 2017 V2 schema standard parameters (54).

Callose deposition analyzed by aniline blue multiphoton microscopy

Sections of leaf and stem of NIa-plants at the PR3 stage were cut and fixed in 4% formaldehyde, faded with 96% alcohol and processed after the addition of SynaptoRed C2

as stated by the manufacturer (Biotium, Fremont, CA, USA), following the methodology described by (55). Multiphoton images were taken with an LSM 880-NLO Axio Imager Z2 microscope (Zeiss, Germany) coupled to a Ti:Sapphire infrared laser (Chameleon Vision II, COHERENT, Scotland). The laser wavelength was set at 723 nm for aniline blue and 800 nm for SynaptoRedC2, both dyes were detected at a 300-685 nm wavelength window with a Non-Descanned Detection.2 (NDD.2) using a 500-550 nm filter (Zeiss, Germany).

DATA AVAILABILITY

The raw reads generated during the current study are publicly available at NCBI under PRJNA844420, PRJNA844411 accession numbers. Materials are available from the corresponding author on reasonable request.

ACKNOWLEDGEMENTS

We thank Gabriela Chávez-Calvillo, Gustavo Rodríguez-Gómez, Domitila J. Rosales, Dalia Rodríguez-Ríos, José N. Santoyo-Villa and Luis J. Saucedo-Vargas and PlanTecc for their technical support. This research was supported by grants from Cinvestav (IP 1995) and Conacyt (4274-N9406). LSR and SLFV supervised the study. LSR, PVM, and AOL designed the experiments. PVM and AOL performed the experiments. PVM analyzed the data and wrote the manuscript. LSR, SLFV and GL edited the manuscript. JPVC directed the in-situ hybridization work performed in 2000. All authors read and approved the final manuscript. The authors declare no conflict of interest.

REFERENCES

1. Nicaise V. 2014. Crop immunity against viruses: outcomes and future challenges. Front Plant Sci 5.
2. Vargas-Mejía P, Vega-Arreguín J, Chávez-Calvillo G, Ibarra-Laclette E, Silva-Rosales L. 2020. Differential Accumulation of Innate- and Adaptive-Immune-Response-Derived Transcripts during Antagonism between Papaya Ringspot Virus and Papaya Mosaic Virus. Viruses 12:230.
3. Wingard SA. 1928. Hosts and symptoms of ring spot, a virus disease of plants. J Agric Res 37:127–153.
4. Bengyella L, Waikhom SD, Allie F, Rey C. 2015. Virus tolerance and recovery from viral induced-symptoms in plants are associated with transcriptome reprograming. Plant Mol Biol 89:243–252.
5. Ghoshal B, Sanfaçon H. 2015. Symptom recovery in virus-infected plants: Revisiting the role of RNA silencing mechanisms. Virology 479–480:167–179.
6. Lindbo JA, Silva-Rosales L, Proebsting WM, Dougherty WG. 1993. Induction of a Highly Specific Antiviral State in Transgenic Plants: Implications for Regulation of Gene Expression and Virus Resistance. The Plant Cell 5:1749–1759.
7. Aregger M, Borah BK, Seguin J, Rajeswaran R, Gubaeva EG, Zvereva AS, Windels D, Vazquez F, Blevins T, Farinelli L, Pooggin MM. 2012. Primary and secondary siRNAs in geminivirus-induced gene silencing. PLoS Pathog 8:e1002941.
8. Santovito E, Mascia T, Siddiqui SA, Minutillo SA, Valkonen JPT, Gallitelli D. 2014. Infection Cycle of Artichoke Italian Latent Virus in Tobacco Plants: Meristem Invasion and Recovery from Disease Symptoms. PLOS ONE 9:e99446.
9. Silva-Rosales L, Lindbo JA, Dougherty WG. 1994. Analysis of transgenic tobacco plants expressing a truncated form of a potyvirus coat protein nucleotide sequence. Plant Mol Biol 24:929–939.
10. Ding S-W, Voinnet O. 2007. Antiviral Immunity Directed by Small RNAs. Cell 130:413–426.

11. Wang X-B, Jovel J, Udomporn P, Wang Y, Wu Q, Li W-X, Gasciolli V, Vaucheret H, Ding S-W. 2011. The 21-Nucleotide, but Not 22-Nucleotide, Viral Secondary Small Interfering RNAs Direct Potent Antiviral Defense by Two Cooperative Argonautes in Arabidopsis thaliana. The Plant Cell 23:1625–1638.

12. Niehl A, Wyrsch I, Boller T, Heinlein M. 2016. Double-stranded RNAs induce a pattern-triggered immune signaling pathway in plants. New Phytologist 211:1008–1019.

13. Pumplin N, Voinnet O. 2013. RNA silencing suppression by plant pathogens: defence, counter-defence and counter-counter-defence. Nat Rev Microbiol 11:745–760.

14. Jaubert M, Bhattacharjee S, Mello AFS, Perry KL, Moffett P. 2011. ARGONAUTE2 mediates RNA-silencing antiviral defenses against Potato virus X in Arabidopsis. Plant Physiol 156:1556–1564.

15. Siddiqui SA, Sarmiento C, Kiisma M, Koivumäki S, Lemmetty A, Truve E, Lehto K. 2008. Effects of viral silencing suppressors on tobacco ringspot virus infection in two Nicotiana species. Journal of General Virology, 89:1502–1508.

16. Kondhare KR, Patil NS, Banerjee AK. 2021. A historical overview of long-distance signalling in plants. Journal of Experimental Botany 72:4218–4236.

17. Myles KM, Wiley MR, Morazzani EM, Adelman ZN. 2008. Alphavirus-derived small RNAs modulate pathogenesis in disease vector mosquitoes. Proceedings of the National Academy of Sciences 105:19938–19943.

18. Fondong VN, Thresh JM, Fauquet C. 2000. Field experiments in Cameroon on cassava mosaic virus disease and the reversion phenomenon in susceptible and resistant cassava cultivars. International Journal of Pest Management 46:211–217.

19. Gasura E, Mukasa SB. 2010. Prevalence and implications of sweetpotato recovery from sweet potato virus disease in Uganda. 4. African Crop Science Journal 18.

20. Lindbo JA, Dougherty WG. 1992. Untranslatable transcripts of the tobacco etch virus coat protein gene sequence can interfere with tobacco etch virus replication in transgenic plants and protoplasts. Virology 189:725–733.

21. Ghoshal B, Sanfaçon H. 2014. Temperature-dependent symptom recovery in Nicotiana benthamiana plants infected with tomato ringspot virus is associated with reduced translation of viral RNA2 and requires ARGONAUTE 1. Virology 456–457:188–197.

22. Martín-Hernández AM, Baulcombe DC. 2008. Tobacco Rattle Virus 16-Kilodalton Protein Encodes a Suppressor of RNA Silencing That Allows Transient Viral Entry in Meristems. Journal of Virology 82:4064–4071.

23. Kørner CJ, Pitzalis N, Peña EJ, Erhardt M, Vazquez F, Heinlein M. 2018. Crosstalk between PTGS and TGS pathways in natural antiviral immunity and disease recovery. 3. Nature Plants 4:157–164.

24. Pooggin MM. 2013. How Can Plant DNA Viruses Evade siRNA-Directed DNA Methylation and Silencing? 8. International Journal of Molecular Sciences 14:15233–15259.

25. Rodríguez-Negrete E, Lozano-Durán R, Piedra-Aguilera A, Cruzado L, Bejarano ER, Castillo AG. 2013. Geminivirus Rep protein interferes with the plant DNA methylation machinery and suppresses transcriptional gene silencing. New Phytologist 199:464–475.

26. Di Serio F, Martínez de Alba A-E, Navarro B, Gisel A, Flores R. 2010. RNA-Dependent RNA Polymerase 6 Delays Accumulation and Precludes Meristem Invasion of a Viroid That Replicates in the Nucleus. Journal of Virology 84:2477–2489.

27. Garcia-Ruiz H, Carbonell A, Hoyer JS, Fahlgren N, Gilbert KB, Takeda A, Giampetruzzi A, Ruiz MTG, McGinn MG, Lowery N, Baladejo MTM, Carrington JC. 2015. Roles and Programming of Arabidopsis ARGONAUTE Proteins during Turnip Mosaic Virus Infection. PLOS Pathogens 11:e1004755.

28. Anandalakshmi R, Marathe R, Ge X, Herr JM, Mau C, Mallory A, Pruss G, Bowman L, Vance VB. 2000. A Calmodulin-Related Protein That Suppresses Posttranscriptional Gene Silencing in Plants. Science 290:142–144.

29. Li F, Huang C, Li Z, Zhou X. 2014. Suppression of RNA Silencing by a Plant DNA Virus Satellite Requires a Host Calmodulin-Like Protein to Repress RDR6 Expression. PLoS Pathog 10.

30. Nakahara KS, Masuta C, Yamada S, Shimura H, Kashihara Y, Wada TS, Meguro A, Goto K, Tadamura K, Sueda K, Sekiguchi T, Shao J, Itchoda N, Matsumura T, Igarashi M, Ito K, Carthew RW, Uyeda I. 2012. Tobacco calmodulin-like protein provides secondary defense by binding to and directing degradation of virus RNA silencing suppressors. Proceedings of the National Academy of Sciences 109:10113–10118.

31. Schwach F, Vaistij FE, Jones L, Baulcombe DC. 2005. An RNA-dependent RNA polymerase prevents meristem invasion by potato virus X and is required for the activity but not the production of a systemic silencing signal. Plant Physiol 138:1842–1852.

32. Medzihradszky A, Gyula P, Sós-Hegedűs A, Szittya G, Burgyán J. 2019. Transcriptome reprogramming in the shoot apical meristem of CymRSV-infected Nicotiana benthamiana plants associates with viral exclusion and the lack of recovery. Molecular Plant Pathology 20:1748–1758.

33. Anjanappa RB, Mehta D, Maruthi MN, Kanju E, Gruissem W, Vanderschuren H. 2016. Characterization of Brown Streak Virus–Resistant Cassava. MPMI 29:527–534.

34. Anjanappa RB, Mehta D, Okoniewski MJ, Szabelska-Beręsewicz A, Gruissem W, Vanderschuren H. 2018. Molecular insights into Cassava brown streak virus susceptibility and resistance by profiling of the early host response. Mol Plant Pathol 19:476–489.

35. Molnár A, Csorba T, Lakatos L, Várallyay É, Lacomme C, Burgyán J. 2005. Plant Virus-Derived Small Interfering RNAs Originate Predominantly from Highly Structured Single-Stranded Viral RNAs. Journal of Virology 79:7812–7818.

36. Nigam D, LaTourrette K, Garcia-Ruiz H. 2020. Mutations in virus-derived small RNAs. 1. Sci Rep 10:9540.

37. Golyaev V, Candresse T, Rabenstein F, Pooggin MM. 2019. Plant virome reconstruction and antiviral RNAi characterization by deep sequencing of small RNAs from dried leaves. 1. Sci Rep 9:19268.

38. Lakatos L, Csorba T, Pantaleo V, Chapman EJ, Carrington JC, Liu Y-P, Dolja V, Fernández L, López-Moya JJ, Burgyán J. 2006. Small RNA binding is a common strategy to suppress RNA silencing by several viral suppressors. The EMBO Journal 25:2768–2780.

39. Valli AA, Gallo A, Rodamilans B, López-Moya JJ, García JA. 2018. The HCPro from the Potyviridae family: an enviable multitasking Helper Component that every virus would like to have. Molecular Plant Pathology 19:744–763.

40. Dougherty WG, Lindbo JA, Smith HA, Parks TD, Swaney S, Proebsting WM. 1994. RNA-mediated virus resistance in transgenic plants: exploitation of a cellular pathway possibly involved in RNA degradation. Mol Plant Microbe Interact 7:544–552.

41. Smith HA, Swaney SL, Parks TD, Wernsman EA, Dougherty WG. 1994. Transgenic plant virus resistance mediated by untranslatable sense RNAs: expression, regulation, and fate of nonessential RNAs. Plant Cell 6:1441–1453.

42. Koltunow AM, Truettner J, Cox KH, Wallroth M, Goldberg RB. 1990. Different Temporal and Spatial Gene Expression Patterns Occur during Anther Development. The Plant Cell 2:1201–1224.

43. Jackson AC. 1992. Detection of rabies virus mRNA in mouse brain by using in situ hybridization with digoxigenin-labelled RNA probes. Molecular and Cellular Probes 6:131–136.

44. Vielle-Calzada J-P, Thomas J, Spillane C, Coluccio A, Hoeppner MA, Grossniklaus U. 1999. Maintenance of genomic imprinting at the Arabidopsis medea locus requires zygotic DDM1 activity. Genes Dev 13:2971–2982.

45. Hetzl J, Foerster AM, Raidl G, Scheid OM. 2007. CyMATE: a new tool for methylation analysis of plant genomic DNA after bisulphite sequencing. The Plant Journal 51:526–536.

46. Fabbro CD, Scalabrin S, Morgante M, Giorgi FM. 2013. An Extensive Evaluation of Read Trimming Effects on Illumina NGS Data Analysis. PLOS ONE 8:e85024.

47. Bray NL, Pimentel H, Melsted P, Pachter L. 2016. Near-optimal probabilistic RNA-seq quantification. Nature Biotechnology 34:525–527.

48. Edwards KD, Fernandez-Pozo N, Drake-Stowe K, Humphry M, Evans AD, Bombarely A, Allen F, Hurst R, White B, Kernodle SP, Bromley JR, Sanchez-Tamburrino JP, Lewis RS, Mueller LA. 2017. A reference genome for Nicotiana tabacum enables map-based cloning of homeologous loci implicated in nitrogen utilization efficiency. BMC Genomics 18:448.

49. Yi L, Pimentel H, Bray NL, Pachter L. 2018. Gene-level differential analysis at transcript-level resolution. Genome Biology 19:53.

50. Tian T, Liu Y, Yan H, You Q, Yi X, Du Z, Xu W, Su Z. 2017. agriGO v2.0: a GO analysis toolkit for the agricultural community, 2017 update. Nucleic Acids Res 45:W122–W129.

51. Shannon P, Markiel A, Ozier O, Baliga NS, Wang JT, Ramage D, Amin N, Schwikowski B, Ideker T. 2003. Cytoscape: A Software Environment for Integrated Models of Biomolecular Interaction Networks. Genome Res 13:2498–2504.

52. Supek F, Bošnjak M, Škunca N, Šmuc T. 2011. REVIGO Summarizes and Visualizes Long Lists of Gene Ontology Terms. PLOS ONE 6:e21800.

53. Axtell MJ. 2013. ShortStack: comprehensive annotation and quantification of small RNA genes. RNA 19:740–751.

54. Dai X, Zhuang Z, Zhao PX. 2018. psRNATarget: a plant small RNA target analysis server (2017 release). Nucleic Acids Res 46:W49–W54.

55. Zavaliev R, Epel BL. 2015. Imaging Callose at Plasmodesmata Using Aniline Blue: Quantitative Confocal Microscopy, p. 105–119. *In* Heinlein, M (ed.), Plasmodesmata: Methods and Protocols. Springer, New York, NY.

FIGURES' LEGENDS

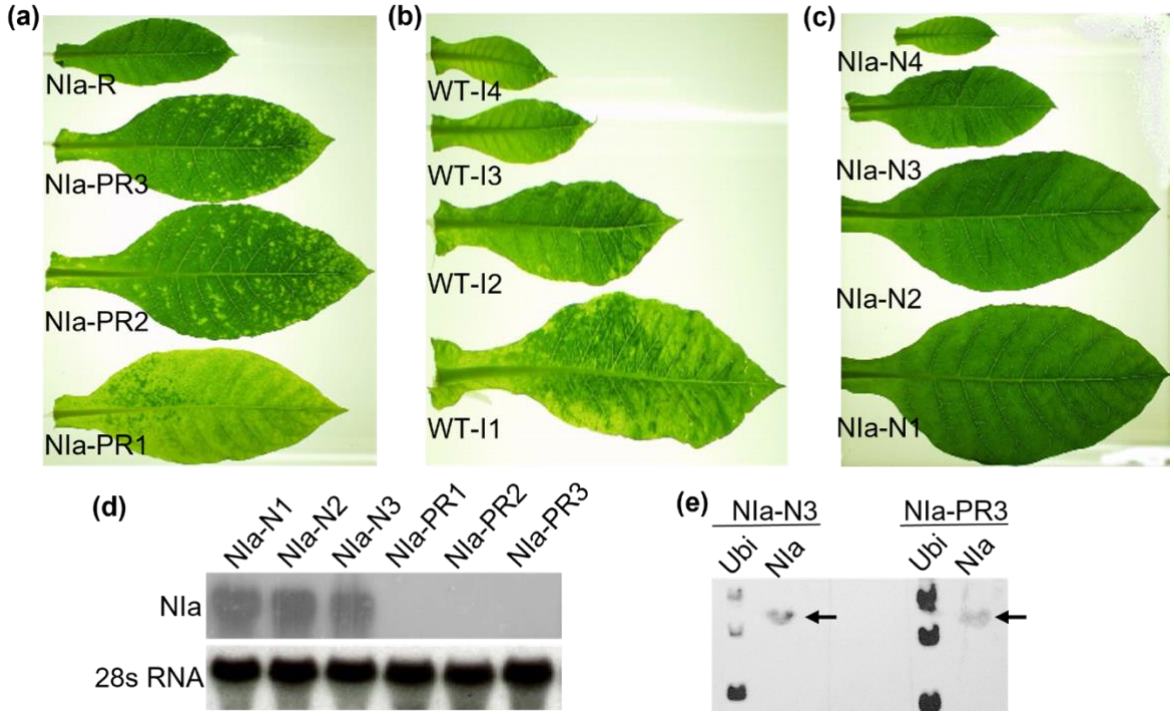

Figure 1: RNA silencing is involved in progressively recovering leaves from NIa plants. **(a)** Inoculated NIa plants in process of recovery (NIa-PR) and fully recovered (NIa-R) **(b)** Inoculated B49 wild-type plants (WT-I). **(c)** The representative phenotype of mock-inoculated NIa plants (NIa-N). **(d)** Northern blot of the NIa viral transgene-derived transcripts and 28S RNA (mostly cytoplasmic) of NIa-N and NIa-PR leaf tissue. **(e)** Run-off assay of the endogenous plant ubiquitin and viral transgene-derived transcripts in the extracted nucleus in leaves of NIa-PR3 and NIa-N3.

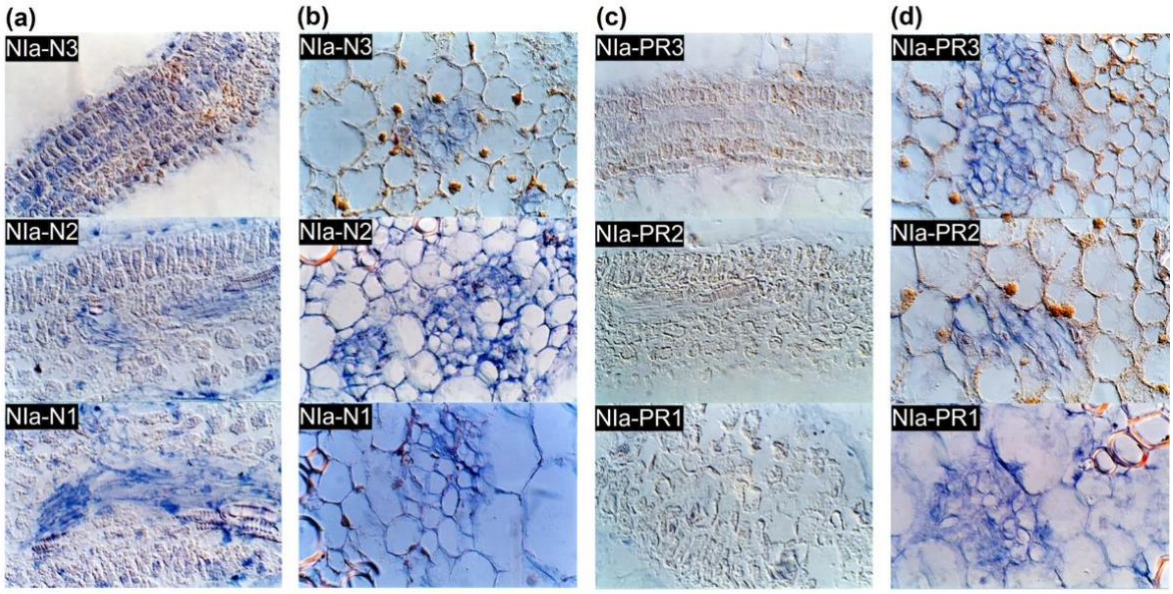

Figure 2: RNA silencing occurred in leaves but not in stems of NIa plants. The presence or absence of TEV-NIa RNA derived from the transgene and/or viral transcript was analyzed by *in situ* hybridization. **(a)** Leaves and **(b)** stems of transgenic mock-infected plants (NIa-N). **(c)** Leaves in process of recovery of transgenic infected plants (NIa-PR) and **(d)** the corresponding sections of their stems.

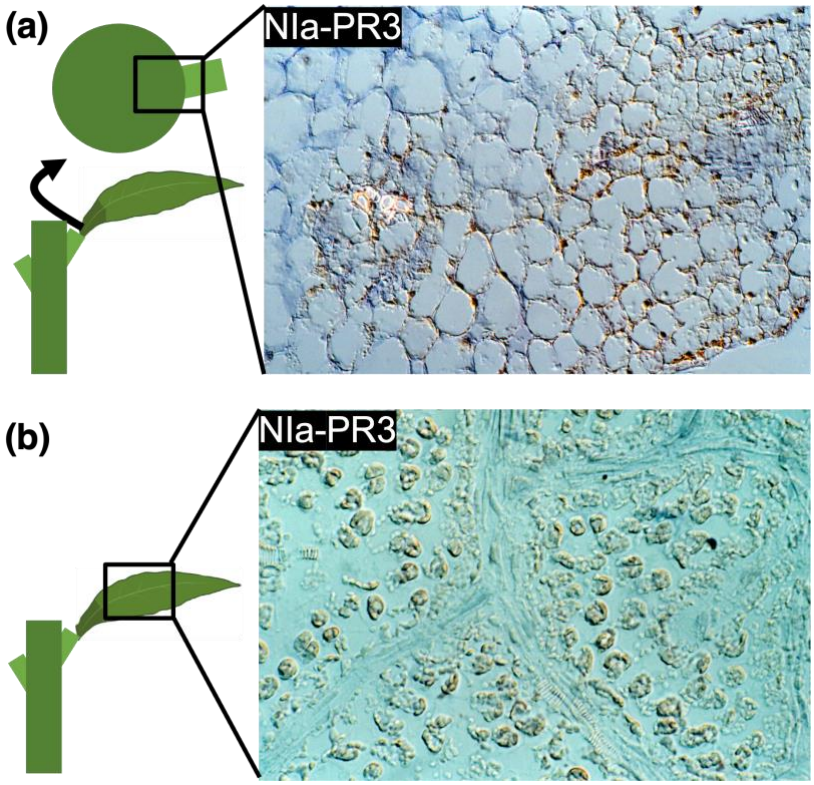

Figure 3: Vicinity between silenced leaf with non-silenced vasculature and non-silenced stem. *In situ* hybridization of RNA of tobacco TEV-NIa plants at the: **(a)** junction of stem-petiole insertion of NIa-PR3 plant and **(b)** leaf section of an NIa-PR3 plant showing non-silenced vasculature and silenced mesophyll cells.

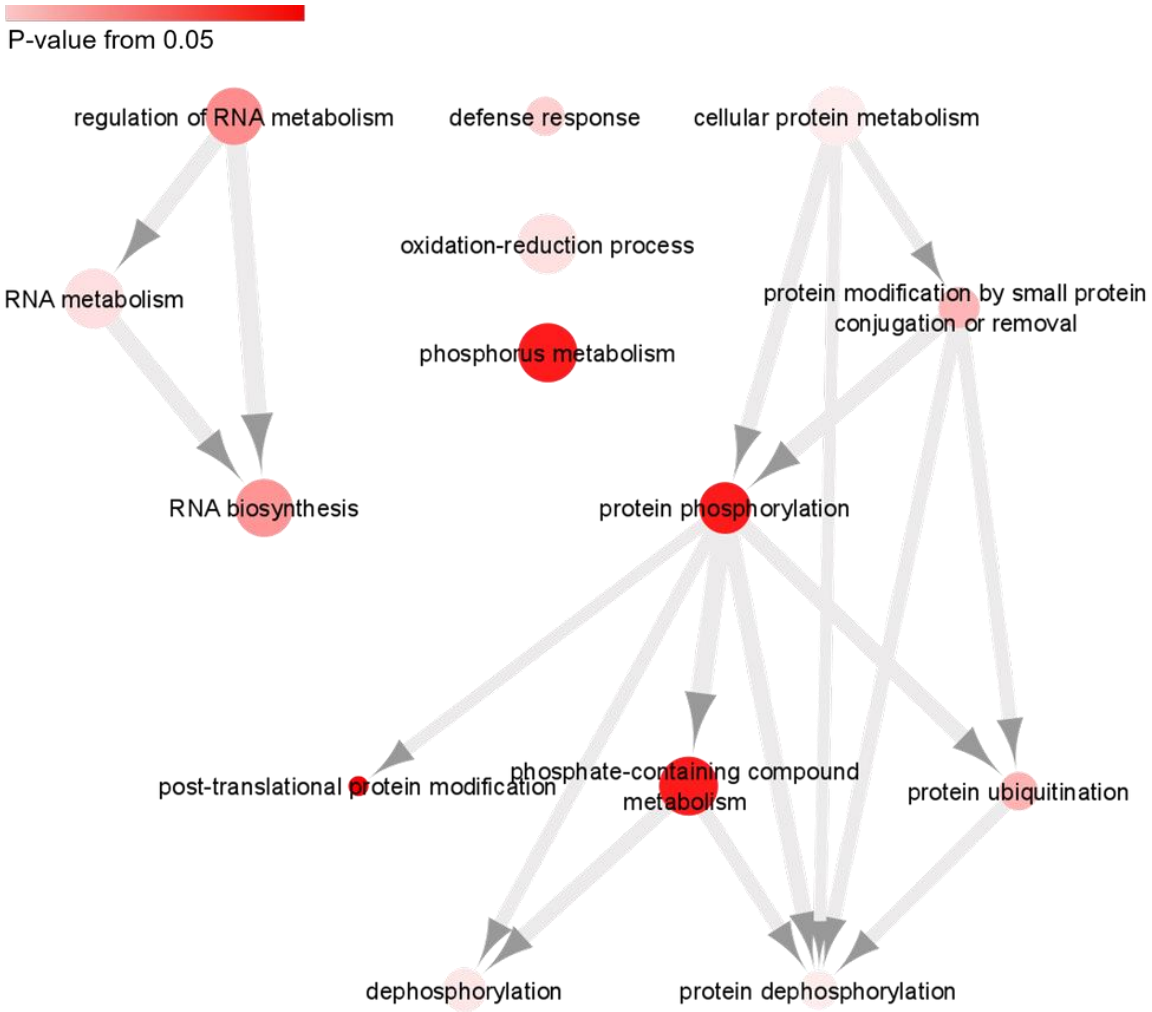

Figure 4: Upregulated biological processes in recovered leaves denoted through a functional DEGs enrichment analysis. Hierarchical network showing biological processes (BP) ontologies. Ontologies shown in the figure are only the semantically reduced terms in REVIGO. Edges represent relationships between the BPs (nodes) and edge weight represent the proportion of genes shared between enrichments. Intensity at node colour indicates the p-value of the enrichment. The node size represents the number of genes at each enrichment.

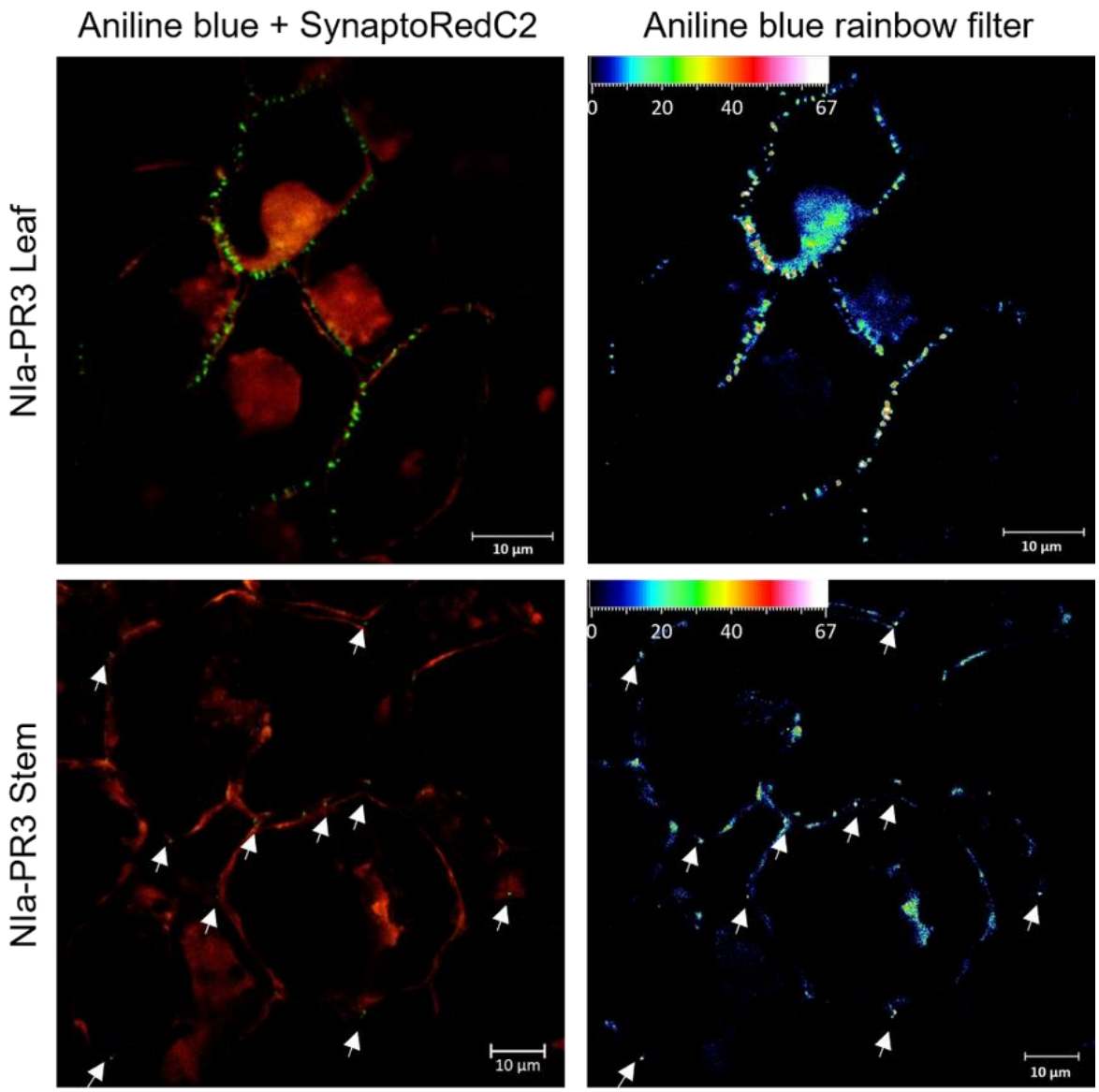

Figure 5: Plasmodesmata callose deposition in NIa-PR3 leaves and stems. Differences in callose deposition were observed with multiphoton imaging of aniline blue fluorescence. The red stain in the images corresponds to SynaptoRedC2 (plasma membrane staining), and the green colour corresponds to aniline blue dye (callose staining). Aniline blue with rainbow filter images was computationally processed to have a metric comparison of callose accumulation. White arrows denote low visibility plasmodesmata callose deposition in the stem. Single-channel images are available in Figure S6.

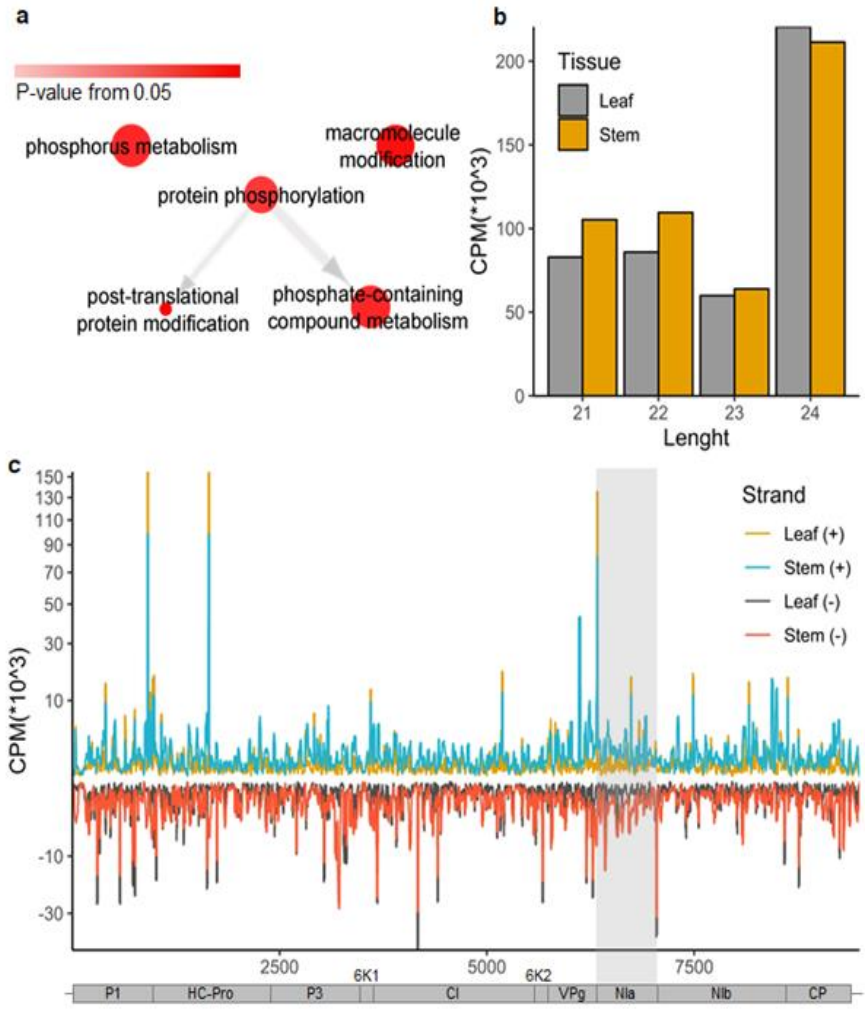

Figure 6: Plant miRNA and vsiRNA profiles in leaves and stem of NIa-PR3 plants. **(a)** Functional enrichment network of Leaf miRNAs. **(b)** Per tissue abundance of 21, 22, 23, and 24 nt vsiRNA. **(c)** TEV genome-wide distribution of vsiRNA in counts per million (CPM).

TABLES

Table 1. Silencing and repressor of gene silencing related DEGs expressed at leaf or stem.

Gene	Log2FC	Tissue
Calmodulin binding protein-like (rgs-CML)	1.58	Stem
Argonaute 1 (AGO1)	1.62	Leaf
Dicer-like 2 (DCL2)	1.95	Leaf

Hua enhancer 1 (HEN1)	1.5	Leaf
RNA-dependent RNA polymerase (RDR6)	2.43	Leaf

Table 2. Callose synthase and deposition at plasmodesmata DEGs expressed in the leaf.

Gene	Log2FC
GLUCAN SYNTHASE-LIKE 12 (GSL12)	4.58
CALLOSE SYNTHASE 1 (CALS1)	2.85
CADMIUM SENSITIVE 1 (CAD1)	2.08
GLUCAN SYNTHASE-LIKE 1 (GSL1)	1.99
IRREGULAR XYLEM 1 (IRX1)	1.43
PENETRATION 3 (PEN3)	1.42
GLUCAN SYNTHASE-LIKE 3 (GSL03)	1.2
UDP-GLUCOSYL TRANSFERASE 74B1 (UGT74B1)	1.17
CELLULOSE SYNTHASE A4 (CESA4)	1.11